# Salinity Effects on the Degree of Hydrophobicity and Longevity for Superhydrophobic Fibrous Coatings

**Fredrick O. Ochanda, Mohamed A. Samaha, Hooman Vahedi Tafreshi, Gary C. Tepper, Mohamed Gad-el-Hak**

*Department of Mechanical & Nuclear Engineering, Virginia Commonwealth University, Richmond, Virginia 23284-3015*

Received 13 July 2011; accepted 9 September 2011
DOI 10.1002/app.35615
Published online 11 December 2011 in Wiley Online Library (wileyonlinelibrary.com).

**ABSTRACT:** Previous studies on submerged superhydrophobic surfaces focused on performance variables such as drag reduction and longevity. However, to use such surfaces for practical applications, environmental factors such as water salinity must be investigated and understood. In this work, experiments were carried out to investigate the impact of salt (sodium chloride, NaCl) concentrations in aqueous solutions on the hydrophobicity and longevity of polystyrene (PS) fibrous coatings. Rheological studies using salt water as a test fluid were performed to determine the effect of salt concentration on drag reduction. Contact-angle measurements were used to validate the results from the rheometer. *In situ* noninvasive optical reflection was used to measure the longevity of the coating—time-dependent loss of entrapped air within the coating—as a function of salinity. The superhydrophobic coating used herein consisted of PS fibers that were deposited using DC-biased AC-electrospinning. Electrospinning is scalable and far less expensive than conventional methods (e.g., microfabrication), bringing the technology closer to large-scale submerged bodies such as submarines and ships. © 2011 Wiley Periodicals, Inc. J Appl Polym Sci 124: 5021–5026, 2012

**Key words:** biomimetic; superhydrophobic coatings; fibers; interfaces; polystyrene; drag reduction

## INTRODUCTION

Surfaces with static contact angle (CA) greater than 150° are typically classified as superhydrophobic. Superhydrophobicity is exhibited in materials with a combination of low surface free energy and micro and/or nanoscale surface roughness. Natural superhydrophobic surfaces are exemplified by lotus leaves, which allow rain drops to roll off of them, carrying dirt away and creating a self-cleaning effect (lotus effect). When fully submersed in water, such a surface can entrap air between the micro/nanostructures resulting in a surface with both air–water and solid–water interfaces. The presence of the air–water interface is responsible for the slip effect, which results in a reduction in the skin-friction drag exerted on the surface.[1]

Synthetic superhydrophobic surfaces have been produced using the same microfabrication techniques developed for the computer industry and typically consist of a regular array of microposts or microridges etc.[2–7] The orientation (with respect to the flow), spacing, and aspect ratio of the microposts or microridges can be adjusted to optimize the generated drag reduction and the stability of the air–water interface (meniscus) against transition from dewetted (Cassie) to wetted (Wenzel) state.[7–9] Many synthetic strategies and materials have been reported for obtaining superhydrophobicity, including sol–gel processing[10] and solution casting,[11] chemical vapor deposition,[12] laser/plasma/chemical etching,[13] lithography,[14] electrical/chemical reaction and deposition,[15] layer-by-layer and self-assembly,[16] and electrospinning.[17] Except for the electrospinning, all of these methods are complicated and require special equipment, high temperature or vacuum conditions, or low-surface-energy material modification involving multiple steps, which makes it difficult for practical applications in large-scale coatings. Electrospinning is a simple, low-cost method that can be used to deposit micro- to nanotextured coatings of a hydrophobic polymer onto substrates of arbitrary geometry. The resulting superhydrophobic surfaces can be applied in diverse applications, including self-cleaning glasses and clothes, protection against corrosion of metallic parts (in bridges, under water constructions etc.), anti-snow sticking, and reducing skin-friction drag in underwater vessels such as submarines. Superhydrophobic coatings can be utilized as a passive method of flow control and may potentially become a viable

*Correspondence to:* M. Gad-el-Hak (gadelhak@vcu.edu).
Contract grant sponsor: Defense Advanced Research Projects Agency (DARPA); contract grant number: W91CRB-10-1-0003.

alternative to the more complex and energy consuming active or reactive flow control techniques such as wall suction/blowing.[18]

The longevity of a submerged superhydrophobic surface depends primarily on the amount of time that air remains trapped within the surface microstructure. In other words, the degree of hydrophobicity and hence the beneficial effects are diminished by the reduction of the amount of air. Recently, several approaches were developed to estimate the longevity of superhydrophobic surface, i.e., the time until transition from dewetted (Cassie) to wetted (Wenzel) state. Bobji et al.[19] used an optical technique to measure how long the surface can entrap air underwater at different pressures by measuring the number of shiny spots that indicates the interface between air and water. Similar studies were performed using a laser beam to investigate the effect of the surface structure on the longevity.[20] Moreover, Poetes et al.[21] used a similar technique for the same test but for different superhydrophobic coatings. Samaha et al.[22] provided a novel optical technique to more accurately measure the longevity of submerged hydrophobic coatings using optical spectroscopy and a pressure vessel. By using their technique, one can measure the longevity of coatings under different environments such as high/low pressure.

In this work, we assess the effect of salt (NaCl) concentration in water on the degree of hydrophobicity and longevity of superhydrophobic polystyrene (PS) spun-fiber coatings as a part of understanding the influence of environmental factors on the performance these simple, low-cost coatings. We developed superhydrophobic fibrous surfaces[17] using recently developed DC biased AC-electrospinning.[23] The degree of hydrophobicity of the coating was estimated via drag-reduction and contact-angle measurements, which used, respectively, a rheometer and a goniometer. The longevity is measured using the aforementioned optical technique.[22]

## EXPERIMENTAL APPROACH

Hydrophobic polymer, PS ($M_n$ = 170,000), was purchased from Sigma–Aldrich Chemicals (St. Louis, MI) and used as received. N,N-Dimethylformamide (DMF) and toluene at high-performance liquid chromatography grade were also obtained from Sigma–Aldrich and were used without further purification. Polymer fibers were fabricated using the DC-biased AC-electrospinning technique. Fibers were electrospun from solutions with 18%, 25%, and 30% weight (wt) PS, but the data reported herein concerns only the last concentration. The polymer was first dissolved in a solvent mixture of DMF and toluene with a 1 : 1 weight ratio. Full details of the experimental procedure to fabricate our superhydrophobic coating are available in our previous work.[17] The electrospun fibers were collected on an aluminum substrate, which was first coated with multipurpose glue to promote adhesion. The surface morphology was determined using a field emission scanning electron microscope (S-70, Hitachi, Japan). Rheological experiments were performed using a rheometer made by Anton Paar Corporation (model Physica MCR 301), equipped with two parallel rotating discs separated by a small fluid-filled gap to measure the stress–strain rate relation. One disc is stationary and attached to a water-cooling system for temperature control.

The second disc rotates at a prescribed speed and is connected to an air bearing to minimize friction. Compressed air at about 6 atm supports the bearing. The rotating disc is connected to a torque-speed measuring system used to calculate the shear stress developed by the fluid and hence drag reduction, and the measured rotational speed is used to calculate the strain rate. The stress–strain rate relation was measured for both superhydrophobic samples as well as smooth control surfaces. The test samples were attached to the stationary disc (bottom plate) and had the same diameter as the rotating disc (top plate) with temperature set at 20 $\pm$ 0.1°C. The test fluids were deionized (D.I.) water and sodium chloride solutions of different concentrations ranging from typical salt concentration in oceans (3.5 wt % NaCl) to 100% salt saturation in water (31 wt % NaCl). The test fluids were dispensed between the top plate and the test substrate attached to bottom plate by pipetting 2.0 mL to fill the gap between them. More details about the setup and mathematical calculations were previously reported by Samaha et al.[22]

The static CAs were measured using a contact-angle ramé-hart goniometer (model number 100-25-A) by placing droplets of deionized water (control) and sodium chloride solutions onto the electrospun surfaces. The salt concentration solutions were the same as in the rheological experiments. Droplets of about 3 μL in volume (diameter of about 1.8 mm) were gently deposited on the substrate using a microsyringe. All measurements were made at five different points for each sample at 20 $\pm$ 1°C. An image of the droplet was taken by an F1 Series Digital Camera and transferred to a PC for contact-angle determination.

The kinetics of air loss from submerged superhydrophobic coatings was measured using an optical spectroscopy system made by Photon Technology International (model Quanta Master™ 30). The intensity of a broad-spectrum white light reflected from the submerged surface was measured as a function of time. As the reflectivity coefficient is greater for the air–water interface than for the solid–water interface, the intensity of the reflected light

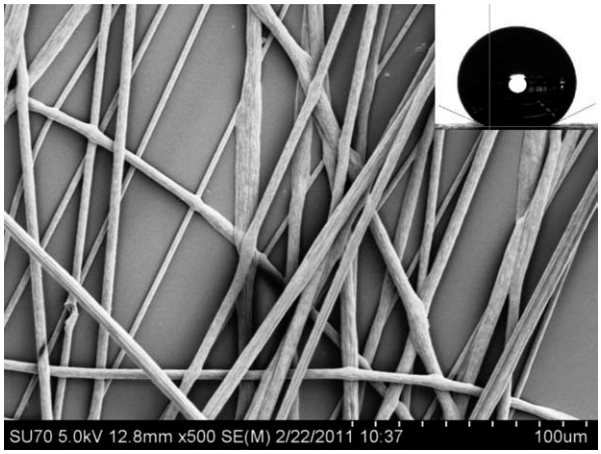


**Figure 1** SEM image of hydrophobic polystyrene (PS) fibers made from 30% polymer solution. Upper right inset shows a water droplet on top of the coating with contact angle of 160°.

decreases as the amount of trapped air decreases. The loss of trapped air will cause a transition from nonwetted (Cassie) state to wetted (Wenzel) state. A detailed description of this apparatus is provided in a previous publication by Samaha et al.[22]

## RESULTS AND DISCUSSION

### Morphology

Making a coating that sturdily sticks to a substrate is essential for practical applications. Without strong adhesion, a coating would separate from its substrate, and hence its beneficial effects would disappear. Equally important is achieving strong adhesion between the different layers of the fibers. Spraying of a thin adhesive polymer film to the metal substrate before electrospinning resulted in a monolayer coating. After electrospinning, it was realized that initial layers of fibers adhered to the metal but subsequent layers did not. By careful control of pump rate and distance between spinneret and metal substrate, the fiber reached the collector when still wet, thus ensuring better adhesion between the different fiber layers. The coating was able to withstand immersion in water for several days during the longevity tests indicating that strong adhesion was achieved.

Figure 1 shows an SEM image of a typical PS micro/nanofiber coating. The inset in the figure shows a water droplet on the coating with a static CA of 160 ±1°, demonstrating the superhydrophobicity of the surface. The diameter of a single PS fiber is a few micrometers and the deposited mat of hydrophobic polymer fibers provides the surface roughness and porosity necessary to entrap air when the surface is immersed in water. As water flows over this surface, the interface between the entrapped air and the water causes very low skin friction, resulting in slip flow and drag reduction. The grid-like arrangement of fibers prevents liquid from penetrating the space (pitch) between fibers, similar to the microposts made by an ordered-microstructure fabrication method. Therefore, the fiber spacing must be close enough (typically micrometers as shown in the figure) to counteract gravitational and other pressures that might cause wetting into the space between the posts. However, if superhydrophobicity is to be achieved, the fraction of the water droplet surface that contacts the low surface energy posts should be much less than the fractional area of the water droplet contacting the air. According to the Cassie–Baxter relation,[24–26] the CA on a composite surface ($\theta_r$) can be expressed as

$$\cos\theta_r = f_1 \cos\theta - f_2 \quad (1)$$

where $f_1$ and $f_2$ represent, respectively, the fractions of solid surface and air in a composite surface (i.e., $f_1 + f_2 = 1$), while $\theta$ is the equilibrium CA on a flat solid surface, which is 96.8° for a smooth PS film. From the equation, the fraction of the PS fibers to the whole apparent surface area is only 0.07, hence the contribution of trapped air is maximized.

### Effect of salinity on hydrophobicity

Sodium chloride solutions of concentration ranging from 3.5 to 31 weight percent in D.I. water were prepared to investigate their effect on the hydrophobicity of the PS fiber coatings. Figure 2 shows the measured drag reduction (using equations demonstrated by Samaha et al.[22]) against strain rate for various water salinity levels. A drag reduction larger than 20% was observed at all NaCl concentrations.

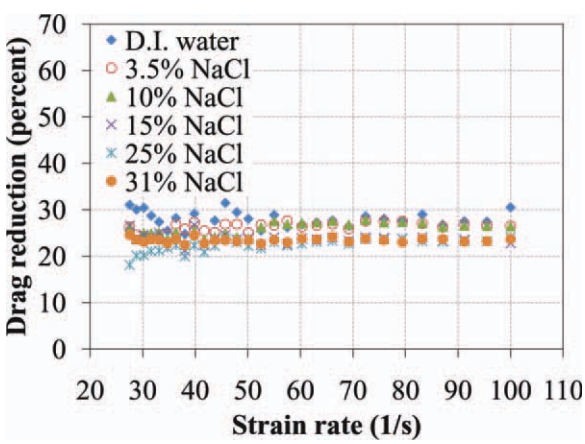


**Figure 2** Rheometer test to estimate drag reduction of PS fibrous coating made from 30% polymer solution with D.I. water and NaCl solutions as test fluids. [Color figure can be viewed in the online issue, which is available at wileyonlinelibrary.com.]

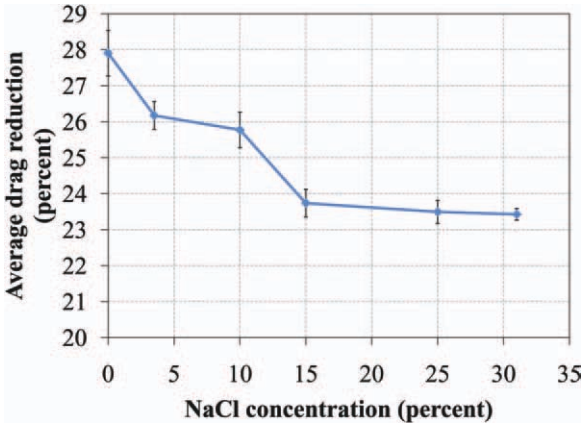


**Figure 3** Effect of salt concentration on average drag reduction of PS fibrous coating. [Color figure can be viewed in the online issue, which is available at wileyonlinelibrary.com.]

Figure 3 is a plot of the drag reduction averaged over the full range of strain rate versus the NaCl concentration and shows a modest decrease in drag reduction with increasing salinity. It should be noted that the estimation of drag reduction depends on the ratio of the wall-shear stress (t) in case of slip to that of no slip.[22] We have repeated the measurements five times for each parameter and it was found that the percentage error in the measured shear stress ($\Delta t/t$) is <1% and this results in not >5% error in drag reduction. Therefore, the experimental uncertainty is far less when compared with the amplitude of the drag reduction reported in this work. We interpret the developed drag reduction to be a result of entrapped air between hydrophobic fibers.

Dynamic viscosities of solutions with different NaCl concentrations have been measured using the rheometer with no-slip moving and stationary discs as shown in Figure 4. It is obvious that the viscosity

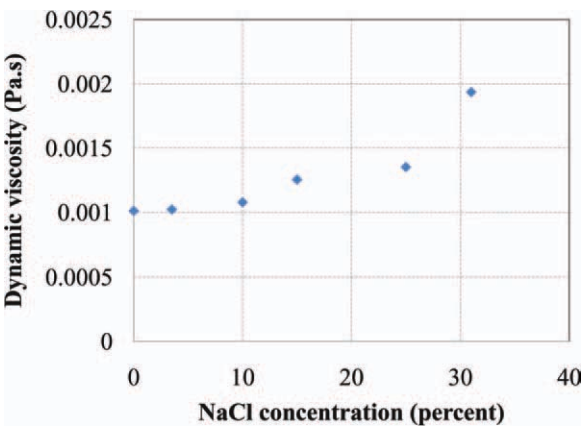


**Figure 4** Variation of dynamic viscosity of NaCl solution as a function of salt concentration. [Color figure can be viewed in the online issue, which is available at wileyonlinelibrary.com.]

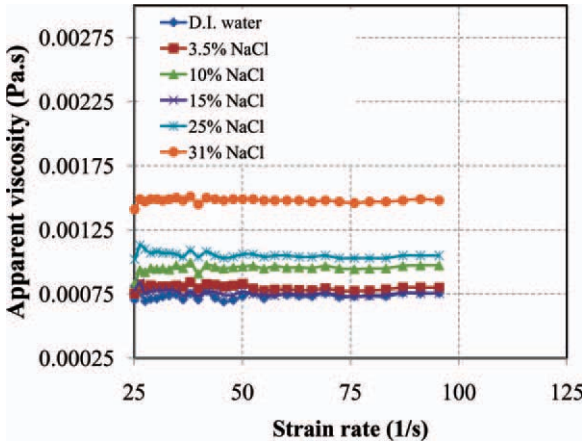


**Figure 5** Apparent viscosity of NaCl solution at different concentrations as a function of strain rate measured for PS fibrous coating. [Color figure can be viewed in the online issue, which is available at wileyonlinelibrary.com.]

of NaCl solution increases with increasing salt concentration until the percentage difference in viscosity relative to that of deionized water reaches 91% at the saturation point. The increase in viscosity on adding ions to liquid water can indeed be explained from the rigid nature of the solvation structure formed by the ion and its first hydration shell.

It is well known[27,28] that when sodium chloride (NaCl) is dissolved in water, it dissociates into positively charged sodium ($Na^+$) and negatively charged chloride ($Cl^-$) ions. The partial positive charge of the hydrogen ends of the water molecules surround the negatively charged chloride ions, and the partial negative charge of the oxygen ends of the water molecules surround the positively charged sodium ions. This effect is thought to result primarily from water molecules directly bonded to the anion and is related to the OH...X bond polarity (where X is a halide, chloride in this case).[29] The amount of hydrogen bonds can be used to characterize the stability of the microstructure of water molecules.[30,31] In general, a larger amount of hydrogen bonds implies stronger intermolecular interactions among the water molecules, which would result in an increase in the viscosity. On the other hand, there is a bulk electrostatic modulation of molecular interactions that originates from the polarization and reorientation of water molecules in the bulk phase. Both electrostatics and solvent-induced forces are modified by the presence of salts,[32] which leads to an increase in the attractive force between the fluid and the surface, i.e., reduces hydrophobicity.

The apparent viscosity—combination of dynamic viscosity and slip effect—increases with increasing NaCl concentration due to an increase in fluid dynamic viscosity and a decrease in generated drag reduction (i.e., surface's hydrophobicity; see Figure 5). For example, if the NaCl concentration increases from

**TABLE I**
**Variation of Specific Gravity as a Function of NaCl Concentration (Percent)**

| NaCl concentration (%) | Specific gravity at 20°C |
|---|---|
| 0.0 | 1.000 |
| 3.5 | 1.026 |
| 10 | 1.074 |
| 15 | 1.112 |
| 25 | 1.193 |
| 31 | 1.247 |

0% to 31%, the apparent viscosity will increase by 103% owing to a percentage increase in dynamic viscosity by 91%, and a relative decrease in drag reduction of 16%. A similar trend has been observed in the specific gravity of the NaCl solution measured at a temperature of 20°C. Table I shows the expected gradual increase in specific gravity of the NaCl solution with increase in concentration, indicating that there is an increase in solution density with concentration when compared with that of pure water.

Contact-angle measurements of droplets with different NaCl concentrations were performed to verify the effect of salinity on hydrophobicity of the fibrous coatings used in the rheometer test. The CA decreased with increasing NaCl concentration in all cases, see Figure 6. The CA data are consistent with the drag-reduction results presented in Figure 3. However, the CA measurements were more sensitive to water salinity and ranged from 160° for pure water to about 143° at 100% salt saturation (31 wt % NaCl). Thus, with increasing concentration of electrolyte, the surface possesses a smaller CA, and less drag reduction, i.e., less hydrophobicity.

Theoretically, NaCl is adsorbed on PS fibers, which can be treated as an interaction of forces including van der waals attractive and electrostatic forces with the former favoring adsorption of $Na^+$ and $Cl^-$ ions on PS surface. In general, the hydrophobicity of a surface and, hence, its hydrophobic force is controlled by changes in surface composition. We reason that the decrease in hydrophobic force in the presence of electrolytes (anion and cation) is due to the adsorption of the ions on the surface.[33,34] This is supported by Gouy–Chapman theory, which predicts that added salt systematically promotes solute adsorption because salt can alter the free energy of forming a charged monolayer with increasing ionic strength.[35]

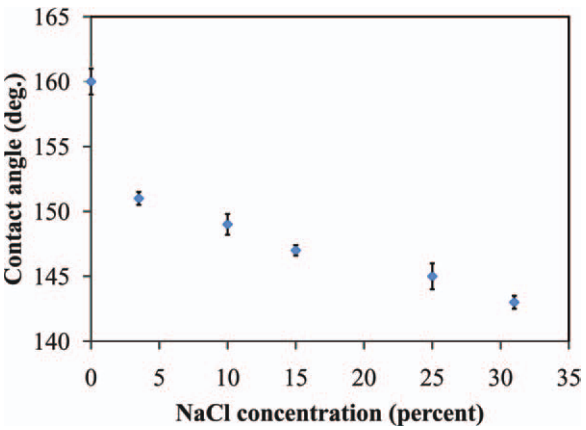


**Figure 6** Effect of NaCl concentration on contact angle of PS fibrous coating. [Color figure can be viewed in the online issue, which is available at wileyonlinelibrary.com.]

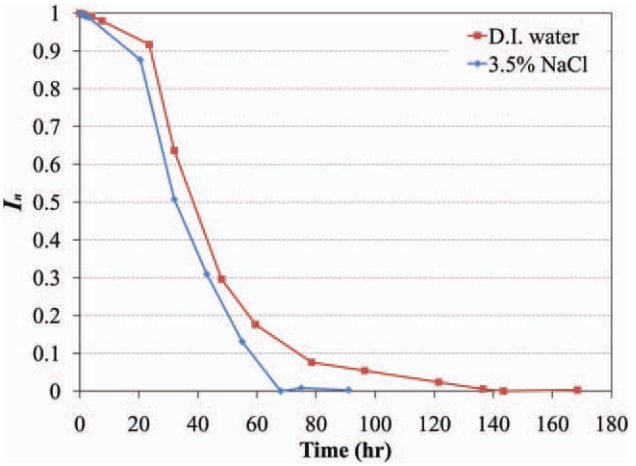


**Figure 7** Effect of salinity on longevity of PS fibrous coating. [Color figure can be viewed in the online issue, which is available at wileyonlinelibrary.com.]

## Longevity studies: salt effects

When a superhydrophobic surface is submerged in water, the spatial distribution of trapped air on its surface exhibits a mirror-like sheen at the air–water interface. Therefore, examining the intensity of reflected light from the surface over time to determine its longevity can monitor the kinetics of loss of the trapped air. We have used light scattering [22] as an indirect, time-dependent measurement of the amount of air trapped within a submerged superhydrophobic fiber surface. The reflected light spectrum was obtained as a function of time and was integrated to obtain wavelength-averaged reflection intensity. Figure 7 shows the normalized average reflected light intensity versus time for two typical samples of the superhydrophobic fibrous coating. One of them was immersed in D.I. water. The other one was immersed in 3.5 wt % NaCl solution (typical salinity of ocean water). The normalized average reflected light intensity, $I_n$, is defined as

$$I_n = \frac{I - I_d}{I_f - I_d} \tag{2}$$

where $I$ is the average integrated measured intensity across the range of wavelengths of visible light, $I_d$ is

the intensity for the completely hydrophilic sample (aged or dead sample), and $I_f$ is the intensity for a new superhydrophobic sample (fresh sample).

It can be seen from Figure 7 that the light intensity decreases with time for both test fluids, which indicates the loss of trapped air and a corresponding reduction in the degree of superhydrophobicity. This effect is believed to be due to the dissolution of air in water.[19,21] Furthermore, it can be seen from the figure that the immersed sample in D.I. water becomes completely hydrophilic after 136 h, whereas the sample submerged in salt water takes only 68 h to become hydrophilic. Therefore, this observation indicates that the onset of wetting or transition from the Cassie state to the Wenzel state starts earlier for samples in salt solution than those in D.I. water. This can be explained by analyzing the parameters that affect the longevity of the surface. First parameter is the rate of air dissolution in water, which decreases with increasing salt concentration.[36] Second, air–water interface is supported by surface tension, which increases by increasing the concentration of NaCl.[37] Finally, as explained in "Effect of salinity on hydrophobicity" section, $Na^+$ and $Cl^-$ ions are adsorbed on the PS surface and the accumulation of positive and negative charges with time leads to decrease in the hydrophobic force and hence reduces surface's longevity. Our results show that although the first and second parameters contribute to increase surface's longevity with adding salt, the effect of the accumulation of charges on the surface dominates and accelerates the transition to the wetted (Wenzel) state. It is worth mentioning that the results of longevity attained using the low-cost fabrication approach used herein are much longer than those reported for ordered-microstructure fabricated surfaces tested in pure water.[19]

## CONCLUSIONS

We performed several experiments to determine how salt (NaCl) concentration in water influenced the hydrophobicity and longevity of PS fibrous coatings. Rheometer tests were provided to determine the effect of salinity on drag-reduction and contact-angle measurements were performed to validate the results obtained from the rheological study. The results show that both drag reduction and static CA (indicating the degree of hydrophobicity) decrease with increasing salt concentration. Moreover, *in situ*, noninvasive optical spectroscopy was performed and showed that the coating longevity was lower for salt water in comparison with D.I. water.

This work demonstrates the effect of water salinity on a superhydrophobic coating. This study opens a pathway for studying more environmental conditions that could affect the performance of superhydrophobic coatings used in practical applications.

## References


1. Rothstein, J. P. Annu Rev Fluid Mech 2010, 42, 89.
2. Ou, J.; Perot, B.; Rothstein, J. P. Phys Fluids 2004, 16, 4635.
3. Ou, J.; Rothstein, J. P. Phys Fluids 2005, 17, 103606.
4. Davies, J.; Maynes, D.; Webb, B. W.; Woolford, B. Phys Fluids 2006, 18, 087110.
5. Maynes, D.; Jeffs, K.; Woolford, B.; Webb, B. W. Phys Fluids 2007, 19, 093603.
6. Daniello, R. J.; Waterhouse, N. E.; Rothstein, J. P. Phys Fluids 2009, 21, 085103.
7. Lee, C.; Choi, C.-H.; Kim, C.-J. Phys Rev Lett 2008, 101, 064501.
8. Lee, C.; Kim, C.-J. Langmuir 2009, 25, 12812.
9. Samaha, M. A.; Tafreshi, H. V.; Gad-el-Hak, M. Phys Fluids 2011, 23, 012001.
10. Shirtcliffe, N. J.; Hale, G.; Newton, H. I.; Perry, C. C. Langmuir 2003, 19, 5626.
11. Erbil, H. Y.; Demirel, A. L.; Avci, Y.; Mert, O. Science 2003, 299, 1377, 15.
12. Love, J. C.; Gates, B. D.; Wolfe, D. B.; Paul, K. E.; Whitesides, G. M. Nano Lett 2002, 2, 891.
13. Fresnais, J.; Chapel, J. P.; Poncin-Epaillard, F. Surf Coat Technol 2006, 200, 5296.
14. Pozzato, A.; Zilio, S. D.; Fois, G.; Vendramin, D.; Mistura, G.; Belotti, M.; Chen, Y.; Natali, M. Microelectron Eng 2006, 83, 884.
15. Shi, F.; Wang, Z. Q.; Zhang, X. Adv Mater 2005, 17, 1005.
16. Zhao, N.; Shi, F.; Wang, Z. Q.; Zhang, X. Langmuir 2005, 21, 4713.
17. Ochanda, F. O.; Samaha, M. A.; Tafreshi, H. V.; Tepper, G. C.; Gad-el-Hak, M. J Appl Polym Sci 2012, 123, 1112.
18. Gad-el-Hak, M. Flow Control: Passive, Active, and Reactive Flow Management; Cambridge University Press: London, United Kingdom, 2000.
19. Bobji, M. S.; Kumar, S. V.; Asthana, A.; Govardhan, R. N. Langmuir 2009, 25, 12120.
20. Sakai, M.; Yanagisawa, T.; Nakajima, A.; Kameshima, Y.; Okada, K. Langmuir 2009, 25, 13.
21. Poetes, R.; Holtzmann, K.; Franze, K.; Steiner, U. Phys Rev Lett 2010, 105, 166104.
22. Samaha, M. A.; Ochanda, F. O.; Tafreshi, H. V.; Tepper, G. C.; Gad-el-Hak, M. Rev Sci Instrum 2011, 82, 045109.
23. Sarkar, S.; Deevi, S.; Tepper, G. Macromol Rapid Commun 2007, 28, 1034.
24. Cassie, A. B. D.; Baxter, S. Trans Faraday Soc 1944, 40, 546, 16
25. Hoefnagels, H. F.; Wu, D.; de With, G.; Ming, W. Langmuir 2007, 23, 13158.
26. Chao-Hua, X.; Shun-Tian, J.; Jing, Z.; Li-Qiang, T.; Hong-Zheng, C.; Mang, W. Sci Technol Adv Mater 2008, 9, 035008.
27. Dillon, S. R.; Dougherty, R. C. J Phys Chem A 2002, 106, 7647.
28. Dougherty, R. C. J Phys Chem B 2001, 105, 4514.
29. Schultz, J. W.; Hornig, D. F. J Phys Chem 1961, 65, 2131.
30. Alenka, L.; David, C. Nature 1996, 379, 55.
31. Hummer, G.; Rasaiah, J. C.; Noworyta, J. P. Nature 2001, 414, 188.
32. Song, J. D.; Ryoo, R.; Jhon, M. S. Macromolecules 1991, 24, 1727.
33. Angarska, J. K.; Dimitrova, B. S.; Danov, K. D.; Kralchevsky, P. A.Ananthapadmanabhan, K. P.; Lips, A. Langmuir 2004, 20, 1799.
34. Christenson, H. K.; Claesson, P. M.; Berg, J.; Herder, P. C. J Phys Chem. 1989, 93, 1472.
35. Persson, C.; Jonsson, A.; Bergstrom, M.; Eriksson, J. C. J Colloid Interface Sci 2003, 267, 151.
36. Millero, F. J.; Huang, F.; Laferiere, A. L. Mater Chem 2002, 78, 217.
37. Jungwirth, P.; Tobias, D. J. J Phys Chem B 2001, 105, 10468.